Journal of Molecular Catalysis B: Enzymatic 70 (2011) 32–40

Contents lists available at ScienceDirect

Journal of Molecular Catalysis B: Enzymatic

journal homepage: www.elsevier.com/locate/molcatb

Kinetic resolution of (±)-1,2-*O*-isopropylidene-3,6-di-*O*-benzyl-*myo*-inositol by lipases: An experimental and theoretical study on the reaction of a key precursor of chiral inositols

Alessandro Bolis Costa Simas[a,*], Angelo Amaro Theodoro da Silva[a,1], Aline Gomes Cunha[b,2], Rafael Silva Assumpção[c,3], Lucas Villas Bôas Hoelz[c,3], Bianca Cruz Neves[b,2], Teca Calcagno Galvão[d,4], Rodrigo Volcan Almeida[b,2], Magaly Girão Albuquerque[c,3], Denise Maria Guimarães Freire[b,**], Ricardo Bicca de Alencastro[b,c,***]

[a] *Universidade Federal do Rio de Janeiro (UFRJ), Centro de Ciências da Saúde (CCS), Núcleo de Pesquisas de Produtos Naturais (NPPN), Bloco H, 1° andar, Laboratório Roderick A. Barnes (Lab. H0-027), Cidade Universitária, 21941-590, Rio de Janeiro, RJ, Brazil*

[b] *UFRJ, Centro de Ciências Matemáticas e da Natureza (CCMN), Instituto de Química (IQ), Programa de Pós-Graduação em Bioquímica, Centro de Tecnologia (CT), Bloco A, 5° andar, Lab. 549-2, Cidade Universitária, 21945-900, Rio de Janeiro, RJ, Brazil*

[c] *UFRJ, CCMN, IQ, Programa de Pós-Graduação em Química, CT, Bloco A, 6º andar, Lab. de Modelagem Molecular (LabMMol), Sala 609, Cidade Universitária, 21941-909, Rio de Janeiro, RJ, Brazil*

[d] *Fundação Oswaldo Cruz (FIOCRUZ), Instituto Oswaldo Cruz (IOC), Centro de Referência Professor Hélio Fraga, Estrada de Curicica n° 2000, Jacarepaguá, 22710-552, Rio de Janeiro, RJ, Brazil*

ARTICLE INFO

Article history:
Received 12 May 2010
Received in revised form
12 December 2010
Accepted 1 February 2011
Available online 5 March 2011

Keywords:
Inositol
Kinetic resolution
Lipase
Molecular modeling
Second tetrahedral intermediate

ABSTRACT

The study on kinetic resolution of two *myo*-inositol derivatives by lipases is reported. Treatment of the tri-ether derivative, (±)-1,2-*O*-isopropylidene-3,5,6-tri-*O*-benzyl-*myo*-inositol, with acylating agents in the presence of different lipases did not afford any detectable amount of acylated products. We speculate that the severe steric hindrance posed by this substrate precluded interaction with the enzymes' catalytic site. Conversely, diol (±)-1,2-*O*-isopropylidene-3,6-di-*O*-benzyl-*myo*-inositol, a key precursor of chiral *myo*-inositol derivatives, bearing one less benzyl protecting group, underwent a successful transesterification in EtOAc, catalyzed by CaL-B (Novozym 435). Thus, monoacetate L-(−)-1,2-*O*-isopropylidene-3,6-di-*O*-benzyl-5-*O*-acetyl-*myo*-inositol was regioselectively formed in >99% *ee*. Additionally, we developed theoretical models of the second tetrahedral intermediate (TI) complex of this reaction to explain the success of the CaL-B and the inactivity of RmL against the same substrate.

Abbreviations: Ac_2O, acetic anhydride; EtOAc, ethyl acetate; Et_2O, diethyl ether; CaL-B, *Candida antarctica* lipase-B; DMAP, 4-dimethylaminopyridine; *ee*, enantiomeric excesses; FT-IR, Fourier transform infra-red spectroscopy; HPLC, high performance liquid chromatography; MS-ESI, mass spectroscopy-electrospray ionization; NMR, nuclear magnetic resonance; PTFE, polytetrafluoroethylene; RmL, *Rhizomucor miehei* lipase; TI, tetrahedral intermediate; TLC, thin-layer chromatography; UV, ultraviolet.

* Corresponding author. Tel.: +55 21 22702683; fax: +55 21 22702683.
** Corresponding author. Tel.: +55 21 25627360; fax: +55 21 25627266.
*** Corresponding author at: UFRJ, Centro de Ciências Matemáticas e da Natureza (CCMN), Instituto de Química (IQ), Programa de Pós-Graduação em Bioquímica, Centro de Tecnologia (CT), Bloco A, 5° andar, Lab. 549-2, Cidade Universitária, 21945-900, Rio de Janeiro, RJ, Brazil. Tel.: +55 21 25627360/21 25627132; fax: +55 21 25627266/21 25627132.
E-mail addresses: abcsimas@nppn.ufrj.br (A.B.C. Simas), amaro.jk@gmail.com.br (A.A.T.d. Silva), alinegc_iq@yahoo.com.br (A.G. Cunha), rafael_bio2004@yahoo.com.br (R.S. Assumpção), lucashoelz@yahoo.com.br (L.V.B. Hoelz), bcneves@iq.ufrj.br (B.C. Neves), teca@ioc.fiocruz.br (T.C. Galvão), volcan@iq.ufrj.br (R.V. Almeida), magaly@iq.ufrj.br (M.G. Albuquerque), freire@iq.ufrj.br (D.M.G. Freire), bicca@iq.ufrj.br (R.B. de Alencastro).
[1] Tel.: +55 21 22702683; fax: +55 21 22702683.
[2] Tel.: +55 21 25627360; fax: +55 21 25627266.
[3] Tel.: +55 21 25627132; fax: +55 21 25627132.
[4] Tel.: +55 21 24486886.

1381-1177/$ – see front matter © 2011 Elsevier B.V. All rights reserved.
doi:10.1016/j.molcatb.2011.02.001

1. Introduction

A major challenge for studies on the synthesis of inositol derivatives, in the context of Medicinal Chemistry and Cell Biology, is the substantial number of steps involved [1–3]. Due to its availability, most of these studies employ *myo*-inositol itself, an achiral cyclitol, as starting material in the synthesis of chiral derivatives. Such strategy usually succeeds because of its practicality and the good repertoire of established protocols for differentiation of the hydroxyl groups in this molecule. Nevertheless, optical resolution of racemic intermediates is required in this case [1,2]. The usual procedure of generating mixtures of diastereomers, to be separated via chromatography or recrystallization, may be practical, but it adds steps and manipulations to the synthetic process, and that leads to decreased overall yields. Thus, the use of enzymes for kinetic resolution of racemic *myo*-inositol derivatives rises up as a valuable alternative.

Lipases, in particular, constitute a class of enzymes of great interest in the field of Biocatalysis applied to Organic Synthesis. These biocatalysts are reputed for their chemical selectivity and specificity [4]. Despite the potential of the use of lipases in chemoenzymatic synthesis of *myo*-inositol, few works have explored it. The number of different *myo*-inositol derivatives assayed as substrates in kinetic resolutions is even smaller. The diether derivative (±)-2,6-di-*O*-benzyl-*myo*-inositol was resolved by means of an immobilized *Candida antarctica* lipase-B (Novozym 435) in vinyl acetate. Thus, L-2,6-di-*O*-benzyl-5-*O*-acetyl-*myo*-inositol was regioselectively produced in 49% yield and 99% enantiomeric excess (*ee*) [5]. A more hindered derivative, 1,2:5,6-*O*-diisopropylidene-*myo*-inositol, was reacted with Ac_2O in Et_2O in the presence of *Candida rugosa* lipase. After a conversion of 48%, L-1,2:5,6-*O*-diisopropylidene-4-*O*-acetyl-*myo*-inositol was formed in moderate *ee* (84%) [6]. In a seminal investigation, the key synthetic precursor (±)-1,2-*O*-cyclohexylidene-*myo*-inositol was reacted with Ac_2O in 1,4-dioxane in the presence of *Pseudomonas sp*. lipase ("Amano" CES lipase). Monoacylated derivative L-2,3-*O*-cyclohexylidene-1-*O*-acetyl-*myo*-inositol was regioselectively produced in 49% yield and 98% *ee* [7,8; see also 9].

In general, all lipases (EC 3.1.1.3) share an evolutionarily conserved structure named α/β-hydrolase folding. In the active site, there is a catalytic triad composed of a nucleophilic residue (Ser) and two residues (Asp/Glu and His) playing the role of a charge relay system [10]. The active site is stabilized by hydrogen bond networks, for each particular enzyme, and the oxyanion hole is usually formed by two backbone nitrogen atoms (NH from the amide groups) close to the nucleophile [10]. Most of the lipases, such as RmL (but not CaL-B), have a structure in alpha-helix named "lid" or "flap" region that covers the active site, which has an important role in the enzyme activity, and a "tunnel" for the substrate recognition, which begins near the catalytic Ser and extends to the vicinity of the "lid" helix [10].

The Ping-Pong Bi–Bi type reaction mechanism, considering a transesterification reaction, is shown schematically in Fig. 1 (in CaL-B and RmL, the catalytic triad residues are numbered as Ser105–His224–Asp187 and Ser144–His257–Asp203, respectively), where EtOAc represents the first substrate and an alcohol (ROH), the second substrate. This reaction also involves two tetrahedral intermediate (TI) complexes, which are related to their correspondent transition states. The first TI complex results from the catalytic-Ser nucleophilic attack on the first substrate, and the second TI complex results from the second substrate nucleophilic attack on the acyl-enzyme complex (*i.e.*, first TI complex) [10]. The literature reports several molecular modeling studies on lipases (*e.g.*, CaL-B), based on classical force fields calculations, but using different approaches such as molecular docking [11], molecular dynamics [12], Monte Carlo [13], and three-dimensional quantitative structure-activity relationship (3D-QSAR) [14].

In the present work, we report the study of lipase-catalyzed optical resolution of two differentially protected racemic *myo*-inositol derivatives (Fig. 3), namely, (±)-3,5,6-*O*-tribenzyl-1,2-*O*-isopropylidene-*myo*-inositol (*rac*-**1**) and (±)-3,6-di-*O*-benzyl-1,2-*O*-isopropylidene-*myo*-inositol (*rac*-**2**). Such compounds (especially *rac*-**2**) are key synthetic intermediates in the synthesis of chiral inositol phosphates or other derivatives [15–21], and had not been previously assayed as substrates for lipases. The methodology used here enables the synthesis of such relevant materials in a cleaner and more efficient manner. In addition, we have docked *rac*-**2** on the CaL-B and RmL active sites, in order to model the second tetrahedral intermediate (TI) complex to explain the structural basis of the CaL-B mediated optical resolution and the inactivity of RmL.

2. Experimental

2.1. General

The synthetic acetylation reaction of product L-**3** was carried out under Ar atmosphere. Unless otherwise noted, commercially available reagents and solvents of analytical grade were used. *Myo*-inositol derivatives *rac*-**1** and *rac*-**2** were prepared according to the literature [22–24]. Ac_2O was treated with P_2O_5 and the mixture was heated at 50–60 °C for 1 h, cooled to room temperature and decanted. After being transferred by cannula to a dry distillation apparatus, the reagent was distilled under Ar. Pyridine was treated with CaH_2 and stirred at room temperature for several hours, and then, the same procedure applied to Ac_2O was carried out. Yields refer to chromatographically and spectroscopically (^{1}H NMR) homogeneous materials.

Reactions were monitored by thin-layer chromatography (TLC), carried out on 0.25 mm E. Merck silica gel plates (60F-254), using UV light as visualizing agent, and/or an aqueous basic solution of $KMnO_4$, and heat as developing agents. E. Merck silica gel (60, particle size 0.040–0.063 mm) was used for flash column chromatography.

NMR spectra were recorded on Bruker DRX-400 and Varian Gemini 200 instruments, and calibrated using residual undeuterated solvent as an internal reference. The following abbreviations were used to explain the multiplicities: s = singlet, d = doublet, t = triplet, q = quartet, m = multiplet, br = broad. IR spectra were recorded on Nicolet Magna 760 FT-IR spectrometer. Elemental analyses were performed on a CHN 2400 unit. Mass spectra (ESI; aq. NH_4Cl sol.) were obtained in a simple quadrupole spectrometer. Specific rotations were recorded on a Jasco DIP-370 polarimeter.

Conversion analyses were carried out via HPLC on a Kromasil-C18 column (40 °C in a CTO-20A oven), eluted (0.5 mL/min) with acetonitrile/H_2O (60:40) by a Shimadzu LC-20AT pump. A Shimadzu SPD-M20A variable-wavelength UV/Vis detector was employed, with the detection set at 215 nm, and the Shimadzu LC solution software was used for chromatogram integration.

Chromatographic determinations of the enantiomeric excesses (*ee*) of L-(−)-**3** were done on the same equipment mentioned above, carrying a Chiralcel OD-H column, and eluted (0.8 mL/min) with hexane/2-propanol (9:1). The samples to be analysed were filtered through a 0.45 μm PTFE filter.

2.2. Enzymes

The commercial immobilized enzymes *C. antarctica* lipase-B (CaL-B, Novozym 435), *Rhizomucor miehei* lipase (RmL, Lipozyme RM IM) and *Thermomyces lanuginosus* lipase (Lipozyme TL IM)

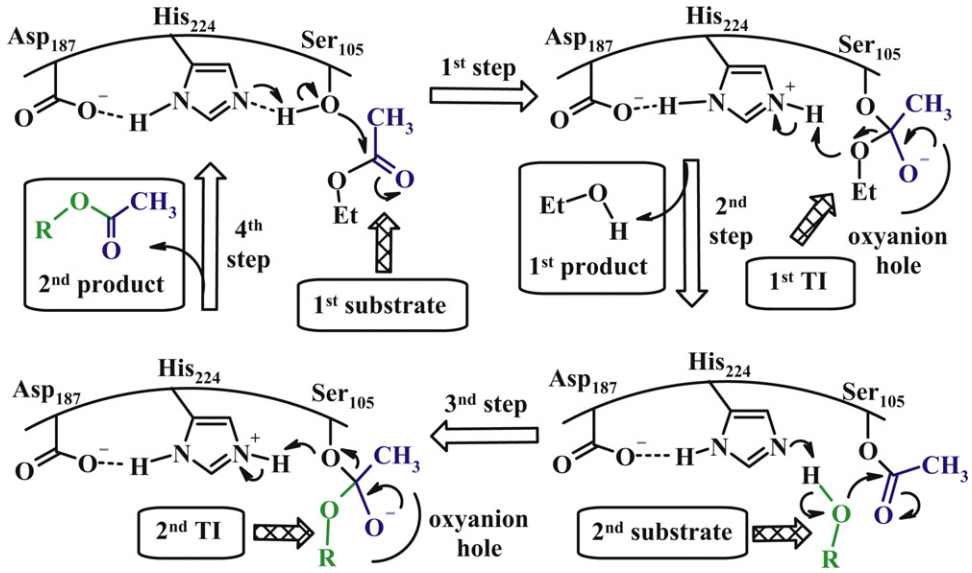

Fig. 1. Schematic general mechanism of lipase-catalyzed reactions, considering a transesterification reaction (catalytic triad numbered as in CaL-B, *i.e.*, Ser105–His224–Asp187; first substrate = EtOAc, second substrate = ROH).

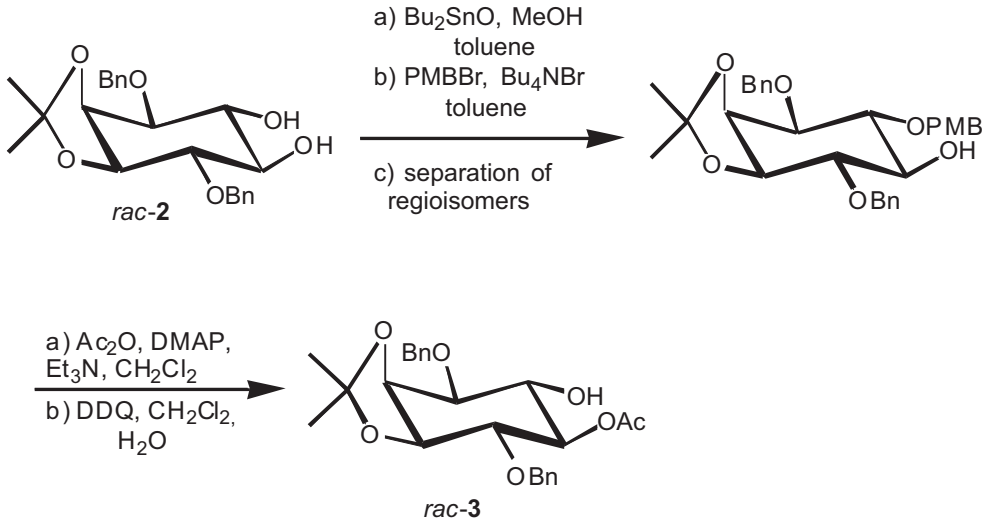

Fig. 2. Synthesis of racemate *rac*-**3**. PMB = *p*-methoxybenzyl group, DDQ = 2,3-dichloro-5,6-dicyanobenzophenone.

were generously provided by Novo. Lipases from *Pseudomonas spp.* ("Amano" PSC II), *C. rugosa* (AY "Amano" 30), *Aspergillus niger* (A "Amano" 12), *Rhizopus javanicus* (F "Amano" AP15), *Rhizopus oryzae* (D "Amano"), *Penicillium camemberti* (G "Amano") and *Pseudomonas fluorescens* (AK "Amano") were obtained from Amano Co. The lipase from *Candida cylindracea* (Lipomod 34) was obtained from Biocatalysts Co.

2.3. Enzymatic reactions and product analysis

The enzymatic reactions were performed at 30 °C for 24 h in closed thermostatized flasks containing *rac*-**1** (0.005 g, 0.010 mmol) or *rac*-**2** (0.005 g, 0.013 mmol), as potential substrates, the lipase (50 mg), with EtOAc (2.5 mL) or a 24:1 hexane/vinyl acetate mixture (for *rac*-**1**) (2.5 mL), 24:1 CH_2Cl_2/acetic anhydride mixture (for *rac*-**2**) (2.5 mL) as acylating mixtures. The reactions were stopped by biocatalyst removal (filtration) and the solvent was evaporated. Under these conditions, no reaction was observed with *rac*-**1**, but *rac*-**2** was able to react with CaL-B in EtOAc, only.

A quantitative experiment of CaL-B-catalyzed resolution of *rac*-**2** (0.040 g; 0.100 mmol) was carried out as outlined above. The produced residue was purified by chromatography (elution with 20:80, 40:60, 60:40 EtOAc/hexane mixtures, sequentially) to afford (-)-1L-5-*O*-acetyl-3,6-di-*O*-benzyl-1,2-*O*-isopropylidene-*myo*-inositol, L-(-)-**3** (0.013 g; 29%), and recovered starting material enriched with enantiomer D-(+)-**2** (0.026 g). (−)-**3**: $[\alpha]_D = -8.1°$ (*c* 0.65, $CDCl_3$); **^{1}H NMR** (400 MHz, $CDCl_3$), δ 1.37 (s, 3H), 1.53 (s, 3H), 2.10 (s, 3H), 3.68–3.75 (m, 2H), 4.05 (t, 1H, J = 8.65 Hz), 4.24 (t, 1H, J = 6.01 Hz), 4.42 (dd, 1H, J = 3.62 5.97 Hz), 4.70–4.84 (m, 4H), 4.89 (t, 1H, J = 8.22 Hz), 7.28–7.41 (m, 10H). ^{13}C NMR (100.62 MHz, $CDCl_3$), δ 21.1, 25.4, 27.4, 70.4, 72.8, 72.9, 73.5, 75.2, 76.9, 78.5, 79.0, 106.5, 127.6, 127.7, 128.1, 128.3, 128.6, 137.8, 138.1, 171.0. **EM-ESI**: m/z = 465.1 $[M+Na]^+$.

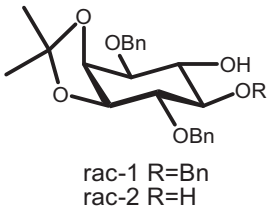

Fig. 3. Differentially protected *myo*-inositol derivatives.

2.4. Acetylation of product L-(−)-3: synthesis of (−)-4

A stirred mixture of hydroxyacetate (−)-**3** (0.023 g; 0.053 mmol) and DMAP (0.0013 g; 0.011 mmol), in pyridine (1.5 mL) at 0 °C, was treated with Ac_2O (0.10 ml; 0.904 mmol) for 15 min, and then, the resulting mixture was warmed to room temperature. After overnight reaction, H_2O was added and the usual aqueous work-up procedure followed. The residue obtained after evaporation of the volatiles was purified by chromatography (elution with 5:95, 20:80 and 35:65 EtOAc/hexane) to furnish L-(−)-**4** (0.022 g; 87%). L-(−)-**4**: $[\alpha]_D = -29.5°$ (*c* 0.95, $CDCl_3$); *lit.* −24.3° [22].

2.5. HPLC analyses

Chromatograms of the reaction mixtures (Reversed-phase HPLC) in the resolution of *rac*-**2** were compared to those of individual samples of *rac*-**2**, *rac*-**3** and *rac*-**4**, showing retention times of 9.3, 15.4, and 26.8 min, respectively. A chemical synthesis of *rac*-**3**, a previously unknown compound, from *rac*-**2**, was devised (Fig. 2). This material was useful in establishing the HPLC methodology for the direct determination of the *ee* of L-(−)-**3**.

For the determination of the *ee* of derivative L-(−)-**3**, on the chiral normal phase, the peaks at 15.7 min (D isomer) and 22.3 min were considered. The enantioselectivity (*E*) was determined according to the work of Chen and colleagues [25] (Eq. (1)).

$$E = \frac{\ln[1 - c \cdot (1 + ee(P))]}{\ln[1 - c \cdot (1 - ee(P))]} \quad (1)$$

2.6. Computational details

2.6.1. General

The molecular mechanics (MM) and the quantum mechanics (QM) calculations were performed with the AMBER v.99 force field and the CNDO semi-empirical method, respectively, as implemented in the HyperChem v.7.5 program [26]. Since the esterification reaction was performed in non-aqueous media (EtOAc is simultaneously the acylating agent and the solvent in this reaction), we did not consider any solvent model in our calculations. The CaL-B (*C. antarctica* lipase-B) and RmL (*R. miehei* lipase) 3D-coordinates, obtained by X-ray diffraction, were retrieved from the Protein Data Bank (PDB) [27], under PDB entry codes 1LBT [28] (resolution: 2.5 Å) and 4TGL [29] (resolution: 2.6 Å), respectively.

2.6.2. Construction of the tetrahedral intermediate complex models

The tetrahedral intermediate (TI) complex models were constructed starting from the coordinates of chain A of CaL-B and RmL enzymes, using the PDB structures 1LBT (the original ligand is methylpenta(oxyethyl)heptadecanoate, T80) and 4TGL (the original ligand is diethyl phosphonate, DEP), respectively. The corresponding original active site ligands (T80 and DEP) were maintained, but all water molecules, non active site ligands, and non-aminoacid structures were removed. The enantiomers in *rac*-**2** were manually docked into the binding site, using the corresponding original active site ligand as reference. Then, if necessary, a careful manual torsion drive and reorientation of each ligand inside the active site were performed in order to obtain the best orientation and to avoid steric clashes, considering the construction of the covalent complex. The original active site ligands were kept only to orientate the superposition of those enantiomers (*rac*-**2**) substrates in the docking procedure but, after that, they were also removed. The catalytic serine residue (Ser105 in CaL-B and Ser144 in RmL) was acetylated by adding an acyl group to the side-chain hydroxyl group, in order to mimic the first TI complex (*i.e.*, acyl-enzyme complex). Subsequently, this complex was modified by making a C–O covalent bond between the carbonyl carbon atom of the Ser-acetyl group and the hydroxyl oxygen atom (C4–OH or C5–OH) of L-**2** and D-**2**, in order to mimic the second TI complex. Hydrogen atoms were added and atom types were assigned with the AMBER force field. This procedure resulted in eight different models of the second TI complex for each enzyme (CaL-B and RmL), according to the nucleophilic attack of each hydroxyl group (C4–OH or C5–OH) of each enantiomer on each face (*Re* or *Si*) of the acetyl group of the acyl-enzyme.

2.6.3. Geometric optimization of the models

Each model of the second TI complex was submitted to a geometric optimization, using the AMBER force field, applying a three-step procedure. In the first step, only the atoms of the former substrate and of the acyl group of the TI complex were optimized, using the steepest-descent (SD) algorithm, to reach a

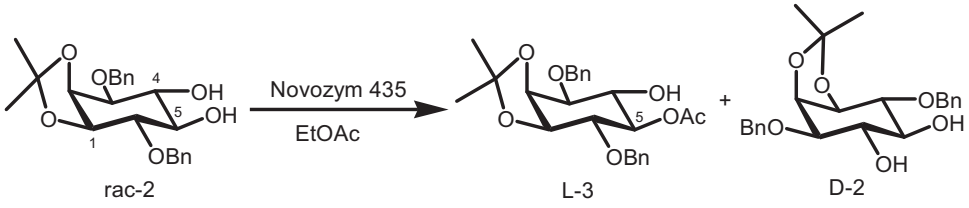

Fig. 4. Kinetic resolution of *rac*-**2** catalyzed by CaL-B in EtOAc.

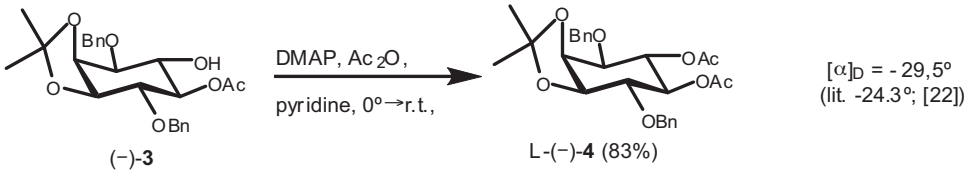

Fig. 5. Acetylation of L-(−)-**3** for determination of configuration.

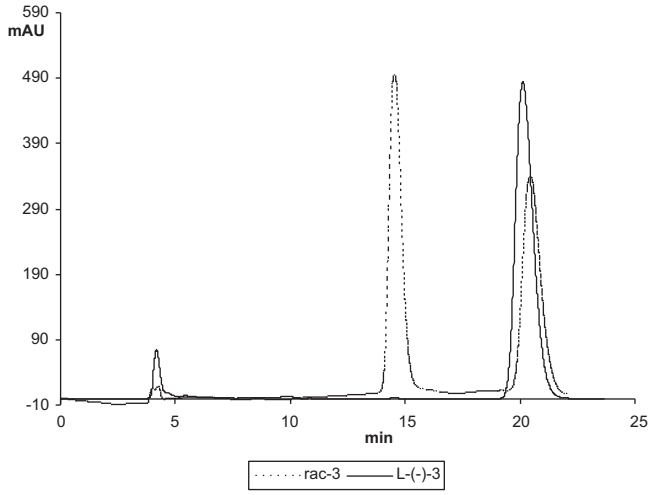

Fig. 6. Chromatograms of *rac*-**3** and product L-(-)-**3** obtained in the resolution of *rac*-**2** catalyzed by CaL-B in EtOAc.

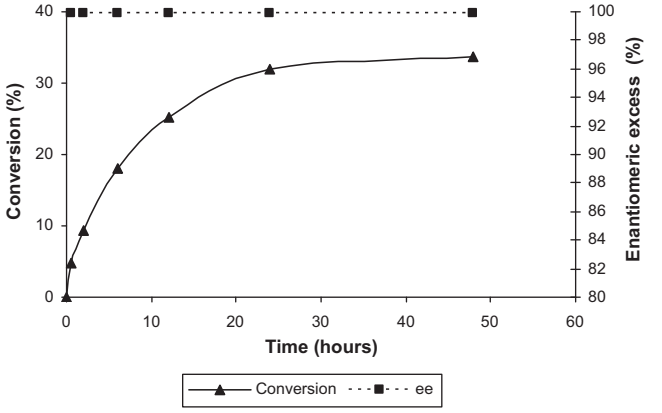

Fig. 7. Time course of conversion and *ee* for the transesterification of *rac*-**2** catalyzed by CaL-B in EtOAc.

root mean square (RMS) gradient lower than 0.6 kcal/mol Å. In the second step, using the same procedure, only the residues within a spherical selection with 9.0 Å of radius centered in the tetrahedral carbon atom from the TI complex were optimized. In the third step, the entire model was optimized, using the conjugate-gradient (CG) algorithm, to reach a RMS gradient lower than 0.1 kcal/mol Å. Subsequently, the partial atomic charges of the residues within the 9.0 Å spherical selection were calculated, using the CNDO semi-empirical model. Finally, this selection was optimized using the AMBER force field, considering the CNDO derived partial atomic charges instead of the bond dipoles, and applying the CG algorithm to reach a RMS gradient lower than 0.1 kcal/mol Å.

3. Results and discussion

3.1. Lipase selection

As pointed out earlier, *myo*-inositol derivatives *rac*-**1** and *rac*-**2** (Fig. 3) had never been assayed before as substrates for lipases. For this task, we chose immobilized commercial lipases CaL-B, RmL [30,31] and several other lipases (see Section 2).

The enantioselective acetylation of *myo*-inositol triether derivative, (±)-3,5,6-tri-*O*-benzyl-1,2-*O*-isopropylidene-*myo*-inositol (*rac*-**1**) (Fig. 3), was attempted in EtOAc or a 24:1 hexane/vinyl acetate mixture. The reaction mixtures were analysed by TLC, but no acylation product was detected. It is likely that the high degree of protection of the hydroxyl groups with bulky benzyl groups in *rac*-**1** made this compound exceedingly sterically hindered, avoiding interaction with the enzymes.

Ling and Ozaki [32] reported that both racemic 3,4,5,6-tetra-*O*-benzyl-*myo*-inositol and a 1-acylated derivative resisted acylation and hydrolysis, respectively, and did not lead to the expected prod-

Table 1
2D-NMR data of L-(−)-**3**[a].

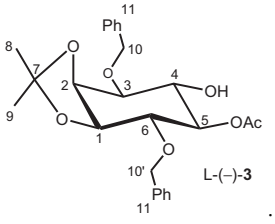

	HSQC		HMBC		COSY
	δ_C	δ_H	$^2J_{CH}$	$^3J_{CH}$	$^2J_{CH}$
CH-1	77.9	4.24	H-2; H-6	–	H-2, H-6
CH-2	73.0	4.42	H-1	H-4	H-1, H-3
CH-3	76.4	3.69	H-2; H-4	H-1; 2H-10	H-2, H-4
CH-4	69.9	4.05	H-3; H-5	H-2	H-3, H-5
CH-5	74.8	4.89	H-4; H-6	H-1	H-4, H-6
CH_3CO-5	171.3	–	CH_3CO-5	H-5	
CH-6	78.5	3.74	H-1; H-5	H-2; 2H-10′	H-1, H-5
C-7	109.6	–	3H-8; 3H-9	H-1	
CH_3-8	24.8	1.37		3H-9	
CH_3-9	26.8	1.53		3H-8	
				H-3 and H-6	
CH_2-10 and -10′	72.32 and 72.37	4.70-4.84			
				($^4J_{CH}$ with H-5)	
OH-4	–	2.61	–	–	
CH_3CO-5	20.6	2.10			

[a] δ_C and δ_H values are in ppm.

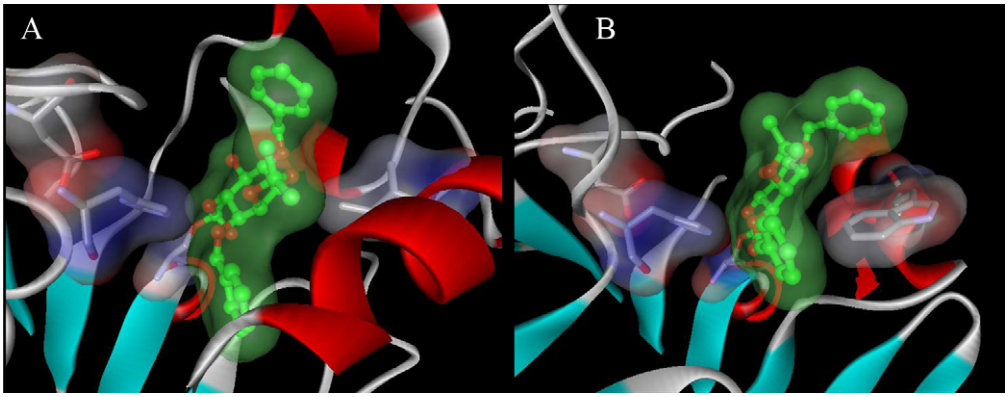

Fig. 8. Models of the second tetrahedral intermediate (TI) complex with CaL-B (A) and RmL (B), showing the putative Trp88 hindrance in the RmL model. The catalytic triad D (Ser105–His224–Asp187 in CaL-B and Ser144–His257–Asp203 in RmL), Ile285 (CaL-B) and Trp88 (RmL) residues are represented in stick models and colored by elements. The remaining residues and all hydrogen atoms were omitted for clarity. Carbon atoms from the *myo*-inositol derivative are colored in green and enzymes are colored by secondary structure. (For interpretation of the references to color in this figure legend, the reader is referred to the web version of the article.)

ucts. This was rationalized as the result of steric hindrance to accessing the active site of the lipases.

Thus, we set out to investigate the use of (±)-3,6-di-*O*-benzyl-1,2-*O*-isopropylidene-*myo*-inositol (*rac*-**2**) (Fig. 3). With one less benzyl protecting group, we expected that this compound would turn out to be a good substrate towards lipases.

We examined the same set of lipases, including CaL-B and RmL, as catalysts in the reaction of *rac*-**2** in neat EtOAc or a 24:1 CH_2Cl_2/acetic anhydride mixture. Only CaL-B was effective in neat EtOAc, leading to a single mono-*O*-acylated product (Fig. 4). Moreover, no diacetylated product was formed, as also determined by HPLC analysis. The chromatogram of the pretreated reaction mixture did not show a peak with the retention time (26.8 min), as would have been the case with a synthetic diacetylated sample.

Hydrolyses of the acetyl derivative of *rac*-**1** and the diacetyl derivative of *rac*-**2** (in hydrated EtOAc or a 1:1 CH_3CN/sodium phosphate buffer mixture (5 mM, pH 7.0)) in the presence of the same lipases (see Section 2) were also briefly investigated. We did not observe any sign of conversion in these reactions.

3.2. Product analysis

The monoacylated product was isolated, purified and characterized by ^1H and ^{13}C NMR. 2D NMR data (Table 1) revealed that the acylation had occurred at the C_5-hydroxyl group to produce compound L-(−)-**3** (Fig. 4).

In order to determine the configuration of product (−)-**3** as L, this compound was converted to diacetate L-(−)-**4** (Fig. 5), a known compound [22]. As the diol derivative, L-**2**, has low specific rotation, the conversion to L-**4** was chosen instead of the hydrolysis to L-**2**. The *ee* of L-(−)-**3** was determined to be >99% by HPLC (Fig. 6).

3.3. Study on time course of conversion and enantiomeric excess (*ee*)

A study on the time course of conversion and *ee* was undertaken (Fig. 7). The maximum conversion was 34% after 48 h. After 24 h, the reaction rate dropped sharply and the conversion remained essentially unaltered thereafter. The enantioselectivity (*E*) was found to be 331. *E* values above 15–30 are considered excellent. It should be emphasized that $E > 200$ cannot be accurately determined due to the significant changes to *E* values following to small variations in *ee*. These may also be caused by experimental errors [33].

3.4. Molecular modeling

To evaluate the structural basis of the CaL-B-mediated optical resolution of *rac*-**2** and the RmL inactivity against the same substrate, we developed theoretical models of the second tetrahedral intermediate (TI) complex of these reactions. We chose RmL as the model of inactivity because of its X-ray structure availability. According to the reaction mechanism (Fig. 1) [10], the enantioselective step of interest in this case is the one that forms the second TI complex, which occurs after the binding of the second substrate (ROH = *rac*-**2**, Figs. 1 and 4).

Since in our reaction model, the second substrate (*rac*-**2**) has two hydroxyl groups (C4–OH and C5–OH, Fig. 4), our approach yielded eight distinct models for each enzyme (CaL-B and RmL), namely, models C4–O–C(*R*), C5–O–C(*R*), C4–OC(*S*), and C5–O–C(*S*) for each enantiomer in *rac*-**2**. Each model corresponds to the second TI complex from the nucleophilic attack of each hydroxyl group (C4–OH or C5–OH) of *rac*-**2** on the *Re* or *Si* face of the Ser-acetyl group (acyl-enzyme), originating a (temporary) stereocenter (*R* or *S*, respectively) at the tetrahedral carbon atom of the second TI complex.

According to our calculations, the most stable model of the second TI complex from CaL-B is the one from the L-**2** substrate (C5–OH as the nucleophilic hydroxyl group and originating a temporary *R* stereocenter), *i.e.* model C5–O–C(*R*) (Fig. 8A), leading to the L-(−)-**3** product, in agreement with our experimental results. In the case of the second TI complex model from RmL (the inactive enzyme against both enantiomers in *rac*-**2**), a visual analysis shows a possible role for Trp88 in the most stable model (Fig. 8B). This residue (Trp88) could be acting as a steric barrier, by impairing the substrate access to the active site, since it belongs to the "lid" helix and partially cover the active site. This observation is in agreement with the results reported by Ema and co-workers [34] in theoretical and kinetic studies on RmL-mediated chiral resolution of relative small secondary alcohols (*e.g.*, 1-phenylethanol, 1-phenyl-2-propanol, and 1-cyclohexylethanol). In the CaL-B TI complex model, a less bulky residue (*i.e.*, Ile285) occupies an almost equivalent spatial position (Fig. 8A).

We should emphasize that these TI complex models were constructed taking into consideration that these substrates have free access to the active site, since we did not model the approximation or the entrance steps of these substrates into the active site. Moreover, as we stated before, CaL-B possesses an open active site, whereas most lipases, such as RmL, contain a "lid" that covers the active sites [10,35].

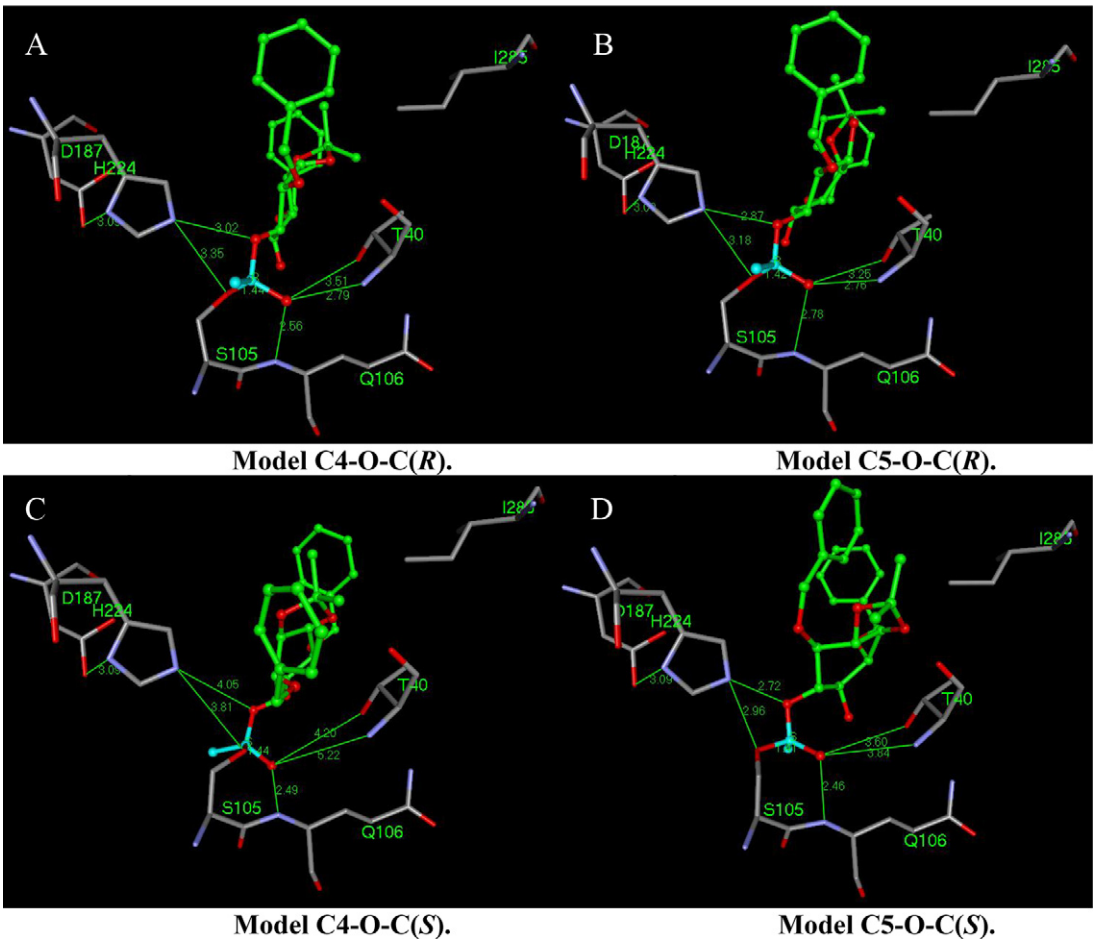

Fig. 9. (A–D) Close view of the second TI complex models between the acetylated CaL-B enzyme (stick model) and L-**2** (ball-and-stick model) substrate, showing residues Thr40 (T40), Ser105 (S105), Gln106 (Q106), Asp187 (D187), His224 (H224), and Ile285 (I285), and selected interatomic distances (Table 2). The remaining residues and hydrogen atoms were omitted for clarity. The amino acid atoms are colored by elements (carbon, gray; oxygen, red; nitrogen, blue). The substrate carbon atoms are colored in green, and the tetrahedral carbon atom of the former acetyl group is colored in cyan. (For interpretation of the references to color in this figure legend, the reader is referred to the web version of the article.)

We should note that our models derived from RmL are based on the X-ray structure (PDB ID: 4TGL) [29] of an open state of this enzyme (*i.e.*, active conformation), where the "lid" is "displaced" to allow the access of the substrate into the active site. However, this displacement may not has been sufficient for substrates larger than the chiral secondary alcohols from Emaĭs group studies, such as *rac*-**2** from the current work. Thus, the main reason for the inactivity of RmL against both enantiomers in *rac*-**2** is still the steric hindrance imposed by Trp88, probably impairing the substrate access to the active site, as discussed above.

Fig. 9 shows the four TI complex models from CaL-B and L-**2**, named C4–O–C(*R*), C5–O–C(*R*), C4–O–C(*S*), and C5–O–C(*S*), and Fig. 10 shows the corresponding graphic of total energy. On models C4–O–C(*R*) and C5–O–C(*R*), the cyclohexane ring of L-**2** shows a regular "chair" like conformation, presenting one axial (at C2) and five equatorial oxygen atoms as in *myo*-inositol itself [36] and its *O*-benzyl derivatives [37,38].

However, on models C4–O–C(*S*) and C5–O–C(*S*), the cyclohexane ring of L-**2** shows distorted "boat" and "envelope" like conformations, respectively, probably due the unfavorable steric interactions of the *O*-benzyl groups of L-**2** with the binding pocket residues of CaL-B. Since the most thermodynamically stable conformation is the "chair" one [39,40], the (temporary) stereocenter at the tetrahedral carbon atom (C*, Table 2) of the second TI complex should have the *R* configuration. Thus, the nucleophilic attack of the substrate hydroxyl group (L-**2**) should necessarily be on the *Re*-face of the Ser-acetyl group.

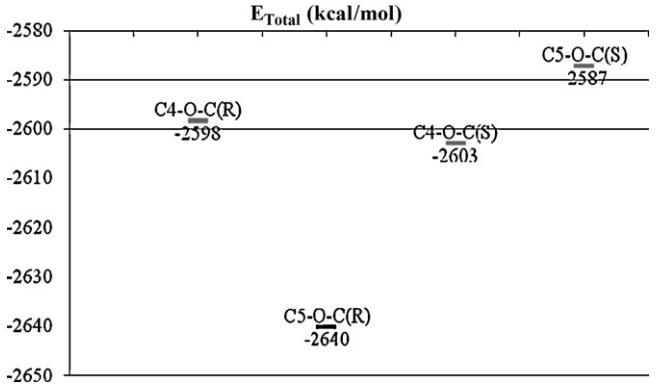

Fig. 10. Total energy (E_{Total}, kcal/mol) of the 2nd TI complex models from the L-**2** (C4–OH or C5–OH) substrate and CaL-B.

Moreover, although the substrate (L-**2**) has two hydroxyl groups (C4–OH and C5–OH), the C5–OH group is the only group acylated by CaL-B. A detailed structural analysis of the four models of the second TI from CaL-B and L-**2** shows a possible explanation for the regioselectivity observed in this reaction. Therefore, Table 2 shows the measured selected interatomic distances (*d1*–*d7*) involving atoms

Table 2
Interatomic distances (*d*, Å) between selected pair of atoms of the second TI complex from the L-**2** substrate, involving the catalytic triad and oxyanion hole residues of CaL-B in the four models.

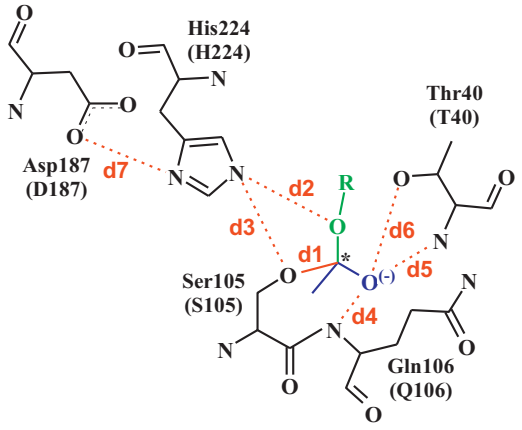

d	Atom 1	Atom 2	Models of the 2nd TI from L-2 (C4–OH or C5–OH)			
			C4–O–C(*R*)	C5–O–C(*R*)	C4–O–C(*S*)	C5–O–C(*S*)
d1	Oγ (Ser105)	C (tetrahedral C*)	1.44 (nd)[a]	1.42 (nd)	1.44 (nd)	1.41 (nd)
d2	Nε2 (His224)	O (substrate)	3.02 (0.02)	2.87 (−0.13)	4.05 (1.05)	2.72 (−0.28)
d3	Nε2 (His224)	Oγ (Ser105)	3.35 (0.37)	3.18 (0.20)	3.81 (0.83)	2.96 (−0.02)
d4	O(−) (oxyanion)	N (Gln106)	2.56 (−0.41)	2.78 (−0.19)	2.49 (−0.48)	2.46 (−0.51)
d5	O(−) (oxyanion)	N (Thr40)	2.79 (0.00)	2.76 (−0.03)	5.22 (2.43)	3.84 (1.05)
d6	O(−) (oxyanion)	Oγ1 (Thr40)	3.51 (1.05)	3.25 (0.79)	4.20 (1.74)	3.60 (1.14)
d7	Oδ2 (Asp187)	Nδ1 (His224)	3.09 (0.10)	3.09 (0.10)	3.09 (0.10)	3.09 (0.10)

[a] The values within parentheses are the deviation values considering the corresponding interatomic distances measure with the original ligand (T80 ester substrate) as reference (deviation values ≥ 1.0 Å are shown in bold). Deviation values for *d1* were not determined (nd) because there is not this correspondent covalent bond between CaL-B and T80.

of the second TI complex models from L-**2** (C4–OH and C5–OH) and atoms of catalytic triad (Ser105–His224–Asp187) and oxyanion hole (Thr40 and Gln106) residues of CaL-B. The deviation values of the corresponding interatomic distances measure with the original ligand (T80 ester substrate) are also shown in Table 2 as reference.

Distance *d1*, as expected, is almost the same in all models (ranging from 1.41 to 1.44 Å, Table 2), since it corresponds to the covalent bond formed between Ser105 and the former acyl group on the first reaction step. Distances *d2*–*d7* are putative hydrogen bonding interactions, which could stabilize the TI and the corresponding transition state. In fact, X-ray structures of lipases (*e.g.*, PDB IDs: 1LBT and 4TGL) [29,30] indicate that the surrounding hydrogen-bonding network maintains the geometry of the catalytic triad, which is important for the stereoselectivity [35]. According to the interatomic distances between the H-bond donor (D) and acceptor (A) atoms, hydrogen bonding interactions (D–H–A) may be classified, in general, as strong (D–A distance = 2.2–2.5 Å), moderate (2.5–3.2 Å), and weak (3.2–4.0 Å) [41]. Thus, Table 2 shows that the best pattern of hydrogen bond network (*d2*–*d7*) is present in model C5–O–C(*R*), followed by models C4–O–C(*R*), C5–O–C(*S*), and C4–O–C(*S*), indicating a better fit of the second TI model C5–O–C(*R*) into the binding pocket of CaL-B.

4. Conclusions

A protocol for kinetic resolution of *myo*-inositol derivative *rac*-**2** was developed. Acetate L-(−)-**3** was formed in good yield and *ee* (>99%). As a matter of fact, *rac*-**2** is the bulkier *myo*-inositol derivative ever to be used in reactions catalyzed by lipases or esterases.

As mentioned before, diol *rac*-**2** may be regarded as one of the most important precursors of inositol phosphates. It displays three differentiated sets of hydroxyl groups, which leads to synthetic flexibility. Our findings suggest a more practical and efficient use of this substance as precursor in enantioselective syntheses of bioactive chiral *myo*-inositols or other derivatives.

Furthermore, the regioselectivity observed in the formation of acetate L-(−)-**3** may be exploited in synthesis as it provides a desirable differentiation of the hydroxyl groups at C4 and C5 [42]. Moreover, by employing protecting group strategies, the acetoxy group at C5 may also be selectively modified.

In addition, molecular modeling studies, using *rac*-**2** as potential substrate of CaL-B and RmL, showed the model leading to the observed product as the most stable model of the second TI complex from CaL-B. This model, *i.e.* C5–O–C(*R*), came from the nucleophilic attack of the C5–OH group of L-**2** on the *Re*-face of the Ser-acetyl group, originating a (temporary) stereocenter (*R*) at the tetrahedral carbon atom. In the case of RmL, even though we were able to model the second TI complex, the model showed a possible steric hindrance imposed by Trp88, which might explain the observed inactivity of RmL against the *rac*-**2** substrates.

Acknowledgements

FAPERJ and CNPq for funding. CAPES for fellowship (AATS). Central Analítica/NPPN and CNRMN/IBM for NMR data. Laboratório de Síntese Orgânica Ambiental (IQ-UFRJ) for polarimetric analyses.

References

[1] K.M. Sureshan, M.S. Shashidhar, T. Praveen, T. Das, Chem. Rev. 103 (2003) 4477–4503.
[2] B.V.L. Potter, D. Lampe, Angew. Chem. Int. Ed. 34 (1995) 1933–1972.
[3] D.C. Billington, Chem. Soc. Rev. 18 (1989) 83–122.
[4] M.L. Gutarra, M.G. Godoy, F. Maugeri, M.I. Rodrigues, D.M. Freire, L.R. Castilho, Bioresour. Technol. 100 (2009) 5249–5254.
[5] K. Laumen, O. Ghisalba, Biosci. Biotechnol. Biochem. 63 (1999) 1374–1377.
[6] S. Chung, Y. Chang, E.J. Lee, B. Shin, Y. Kwon, K. Kim, D.H. Lee, M. Kim, Bioorg. Med. Chem. Lett. 8 (1998) 1503–1506.
[7] L. Ling, Y. Watanabe, T. Akiyama, S. Ozaki, Tetrahedron Lett. 33 (1992) 1911–1914.
[8] L. Ling, S. Ozaki, Carbohydr. Res. 256 (1994) 49–58.
[9] P. Andersch, M.P. Schneider, Tetrahedron: Asymmetry 4 (1993) 2135–2138.
[10] W. Hide, L. Chan, W. Li, J. Lipid Res. 33 (1992) 167–178.

[11] P.B. Juhl, P. Trodler, S. Tyagi, J. Pleiss, BMC Struct. Biol. 9 (2009) 39.
[12] I. Vallikivi, L. Fransson, K. Hult, I. Jarving, T. Pehk, N. Samel, V. Tougu, L. Villo, O. Parve, J. Mol. Catal. B: Enzym. 35 (2005) 62–69.
[13] E.B. De Oliveira, C. Humeau, L. Chebil, E.R. Maia, F. Dehez, B. Maigret, M. Ghoul, J.M. Engasser, J. Mol. Catal. B: Enzym. 59 (2009) 96–105.
[14] P. Braiuca, K. Lorena, V. Ferrario, C. Ebert, L. Gardossi, Adv. Synth. Catal. 351 (2009) 1293–1302.
[15] T. Desai, J. Gigg, R. Gigg, E. Martín-Zamora, Carbohydr. Res. 262 (1994) 59–77.
[16] T. Desai, J. Gigg, R. Gigg, E. Martín-Zamora, Carbohydr. Res. 296 (1996) 97–133.
[17] W. Li, C. Schultz, J. Llopis, R.Y. Tsien, Tetrahedron 53 (1997) 12017–12040.
[18] A. P. Kozikowski, P. Dennis, H. Sun, J. Brognard, WO 2004022569 (2004).
[19] S. Ballereau, P. Guedat, S.N. Poirier, G. Guillemette, B. Spiess, G. Schlewer, J. Med. Chem. 42 (1999) 4824–4835.
[20] A. Rajindra, US 6232486 (2001).
[21] S.J. Conway, G.J. Miller, Nat. Prod. Rep. 24 (2007) 687–707.
[22] T. Desai, J. Gigg, R. Gigg, E. Martín-Zamora, N. Schnetz, Carbohydr. Res. 258 (1994) 135–144.
[23] A.B.C. Simas, K.C. Pais, A.A.T. da Silva, J. Org. Chem. 68 (2003) 5426–5428.
[24] A.B.C. Simas, A.A.D. Silva, T.J. dos Santos Filho, P.T. Barroso, Tetrahedron Lett. 50 (2009) 2744–2746.
[25] C.S. Chen, Y. Fujimoto, G. Girdaukas, C.J. Sih, J. Am. Chem. Soc. 104 (1982) 7294–7299.
[26] HyperChem Release 7.5, HyperCube Inc., 1115 NW 4th St., Gainesville, FL 32601, USA, 2003.
[27] H.M. Berman, J. Westbrook, Z. Feng, G. Gilliland, T.N. Bhat, H. Weissig, I.N. Shindyalov, P.E. Bourne, Nucleic Acids Res. 28 (2000) 235–242.
[28] J. Uppenberg, N. Ohrner, M. Norin, K. Hult, G.J. Kleywegt, S. Patkar, V. Waagen, T. Anthonsen, T.A. Jones, Biochemistry 34 (1995) 16838–16851.
[29] U. Derewenda, A.M. Brzozowski, D.M. Lawson, Z.S. Derewenda, Biochemistry 31 (1992) 1532–1541.
[30] V. Gotor-Fernández, R. Brieva, V. Gotor, J. Mol. Catal. B: Enzym. 40 (2006) 111–120.
[31] V. Kiss, G. Egri, J. Bálint, I. Ling, J. Barkóczi, E. Fogassy, Tetrahedron: Asymmetry 17 (2006) 2220–2234.
[32] L. Ling, S. Ozaki, Bull. Chem. Soc. Jpn. 68 (1995) 1200–1205.
[33] V.E.U. Costa, H.L.N. de Amorim, Quim. Nova 22 (6) (1999) 863.
[34] T. Ema, J. Kobayashi, S. Maeno, T. Sakai, M. Utaka, Bull. Chem. Soc. Jpn. 71 (1998) 443–453.
[35] G.H. Peters, O.H. Olsen, A. Svendsen, R.C. Wade, Biophys. J. 71 (1996) 119–129.
[36] A. Bonnet, W. Jones, W.D.S. Motherwell, Acta Crystallogr. E62 (2006) o2902–o2904.
[37] I.D. Spiers, C.H. Schwalbe, S. Freeman, Acta Crystallogr. C52 (1996) 2575–2578.
[38] V. Graingeot, C. Brigando, D. Benlian, Acta Crystallogr. C52 (1996) 2283–2285.
[39] V.I. Shvets, Russ. Chem. Rev. 43 (1974) 488–502.
[40] R.F. Irvine, M.J. Schell, Nat. Rev. Mol. Cell Biol. 2 (2001) 327–338.
[41] G.A. Jeffrey, An Introduction to Hydrogen Bonding, Oxford University Press, New York and Oxford, 1997.
[42] (a) J. Gill, R. Gigg, E. Martin-Zamora, Tetrahedron Lett. 34 (1993) 2827–2830;
(b) J.L. Offer, H.P. Voorheis, J.C. Metcalfe, G.A. Smith, J. Chem. Soc., Perkin Trans. 1 (1992) 953;
(c) Ref [19], which deals with synthesis of fluoro-myo-inositol, complements Ref. [42(b)].